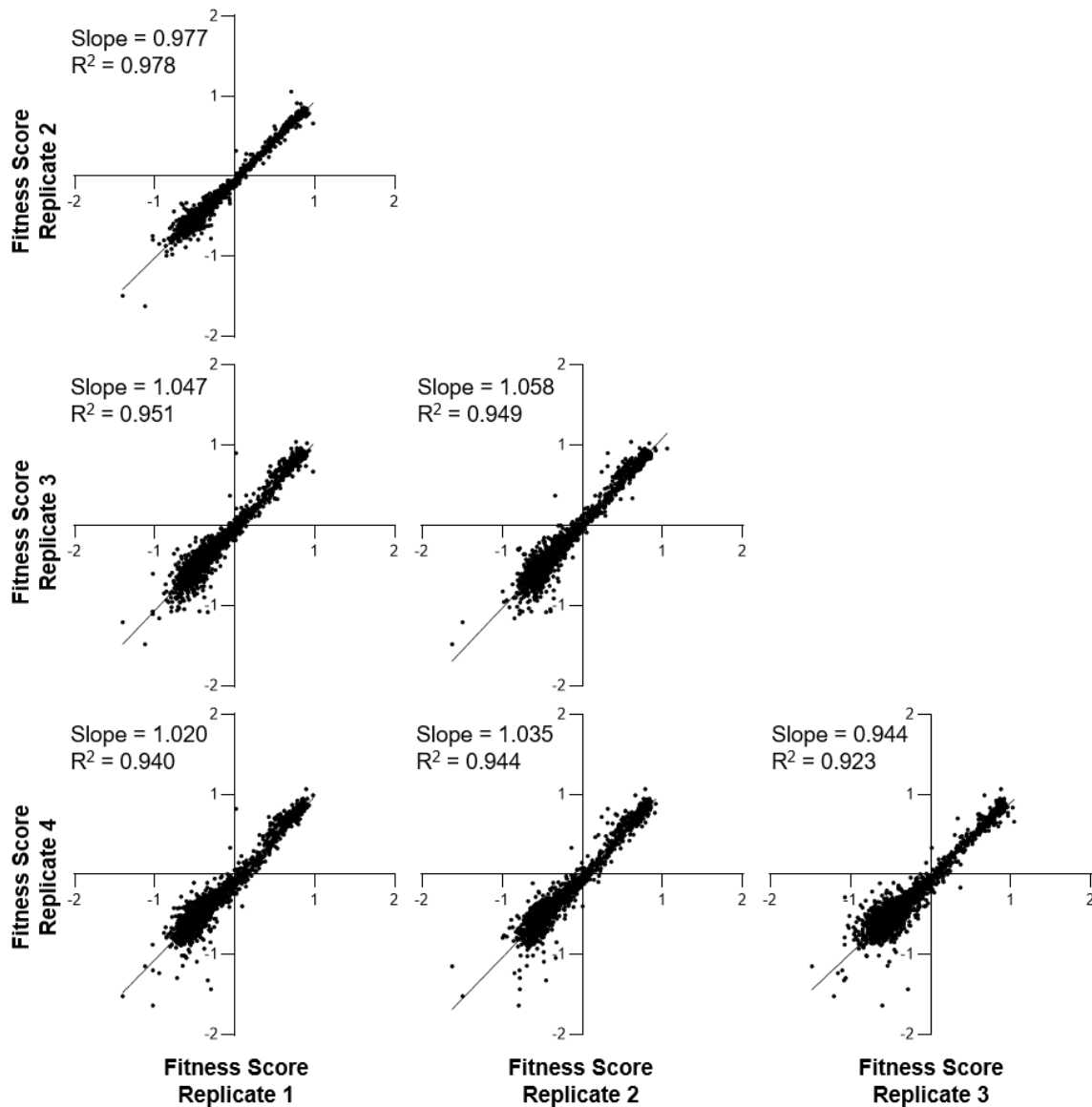


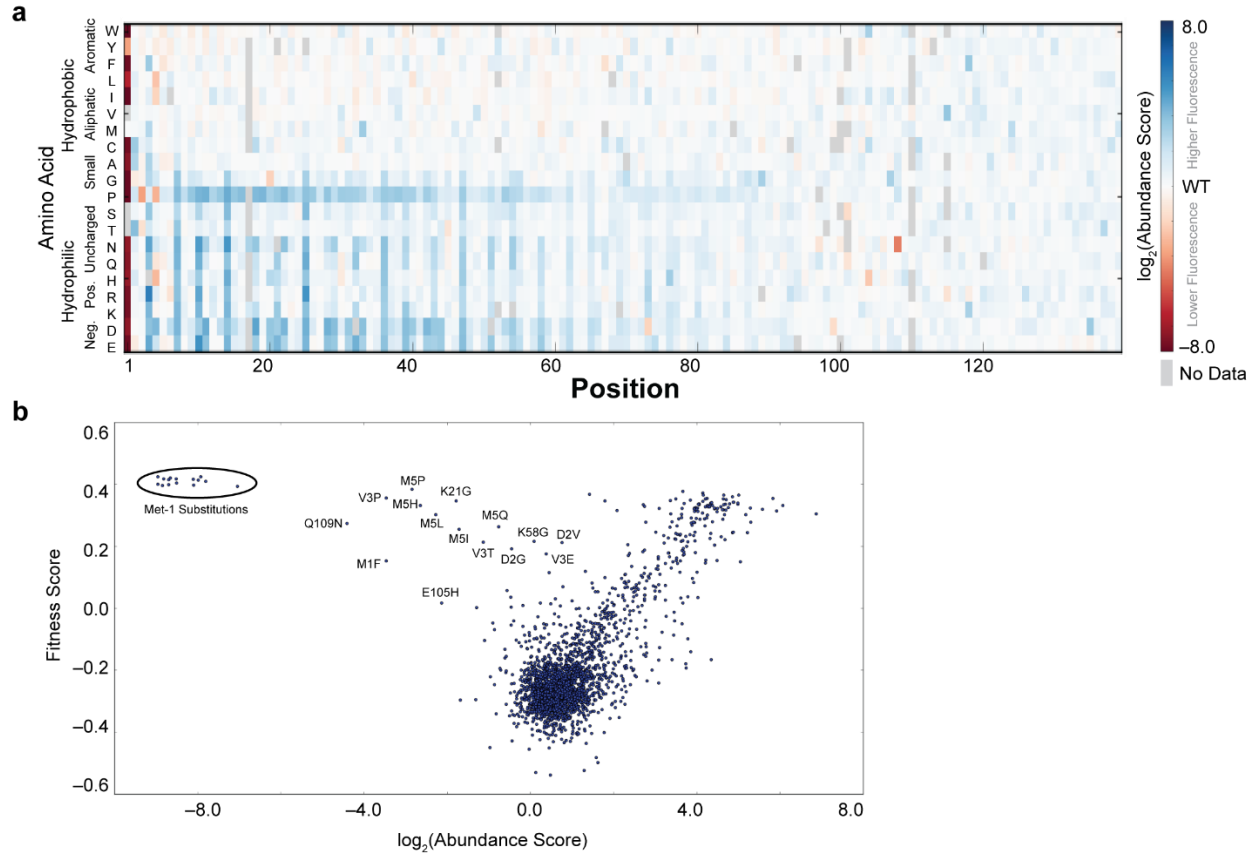
SUPPLEMENTARY INFORMATION

Deep Mutational Scanning Reveals the Structural Basis for α -Synuclein Activity

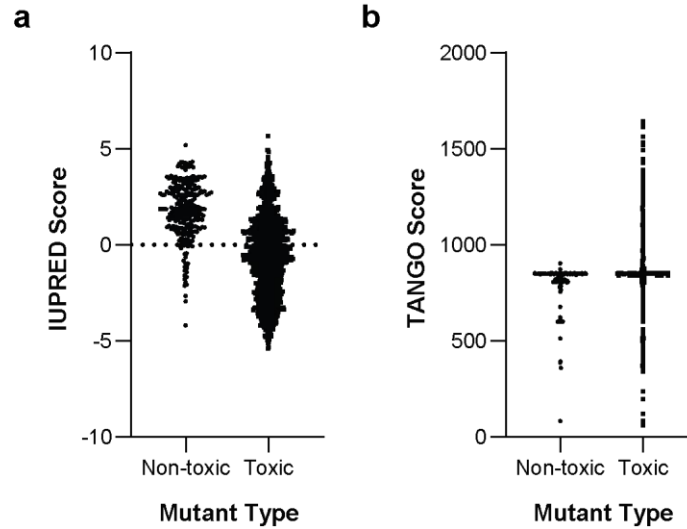
Robert W. Newberry, Jaime T. Leong, Eric D. Chow, Martin Kampmann, William F. DeGrado



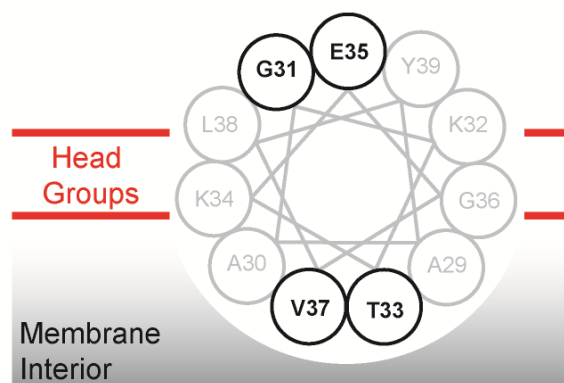
Supplementary Fig. 1 | Correlation of fitness scores between replicates. Details of linear regressions are shown.



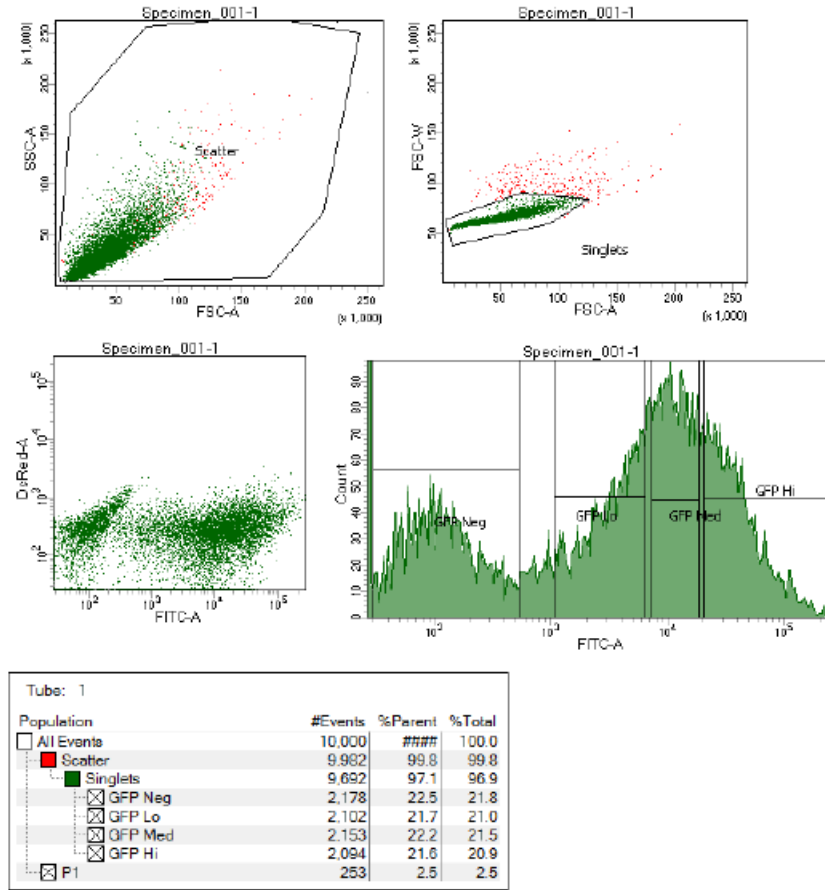
Supplementary Fig. 2 | Expression level of α -synuclein variants. **a**, Abundance scores (the ratio of frequencies in high- and low-GFP bins, normalized to WT) for expression of α -synuclein-GFP variants in yeast. **b**, Correlation of expression level and toxicity for expression of α -synuclein-GFP variants in yeast.



Supplementary Fig. 3 | Computed biophysical properties of α -synuclein variants. Disorder propensity and aggregation propensity of α -synuclein variants calculated by IUPred⁴⁹ and TANGO⁵⁰, respectively. Variants were divided into toxic (n=2335) and non-toxic (n=265) mutants based on the minimum in the distribution of fitness scores; mutants with fitness scores less than or equal to the fitness score with the fewest representatives were considered toxic, and mutants with fitness scores greater than the fitness score with the fewest representatives were considered toxic. While the difference in means between these two groups is small for TANGO scores (797.2 vs 843.5, $P = 8.2 \times 10^{-10}$, one-sided student's T-test), it is dramatic for IUPred scores (1.798 vs -0.5955, $P = 1.8 \times 10^{-77}$, one-sided student's T-test). From these data, we conclude that (1) amyloid formation contributes minimally to toxicity in yeast and (2) the conformational state that drives toxicity is ordered.



Supplementary Fig. 4 | Spatial relationship of selected α -synuclein residues with the membrane surface.



Supplementary Fig. 5 | Overview of the flow cytometry strategy and data collection.